accepted at the AUV 2000,
published at the OCEANS 2000, Providence, U.S.A

Robust tracking under uncertainties

Christfried Webers & Uwe R. Zimmer

GMD - Japan Research Laboratory
AIM Building 8F, 3-8-1, Asano, Kokurakita-ku
Kitakyushu-city, 802-0001, Japan
http://www.gmd.gr.jp/

Robust tracking of vehicles under uncertain, noisy, and discontinuous positioning is a significant part of autonomous navigation in unknown environments. This article suggests two methods for track control, where the initial parameters of the on-line control are physically explainable, the resulting track as well as the control parameters are asymptotically converging and glitches in the localization are handled robustly. Practical experiments with landbound vehicles show the reliability and limitations of the method in various environments in setups for following simple attractors. Due to the physical meaning of the control parameters the adaptation to changed kinematic or dynamics is significantly simplified.

Keywords: **mobile robots, tracking, dynamical environments, exploration, self-localization, robust control**

1. Motivation

A common task in mobile robotics is to drive the robot to a certain position and orientation as fast as possible and within the limits of the static and dynamic properties of the robot setup. Autonomous robots may not only choose targets which are not smoothly connected, but the choice itself may not be predictable any more. Therefore, a robust beheaviour in reaching noisy, drifting, or even stochastically moving targets is a necessary condition for successfull applications with autonomous robots.

Because autonomous systems have only approximate information about the environment via their sensory system, continuous corruptions and corrections of the position measurement appear on the motion control level in the same way as purposefully moved targets. In that sense, robust posing control represents always a target following problem.

One Lyapunov based approach ([2], [7], [8]) and one superimposed dynamics approach are employed to study the dynamic behaviour of a physical land robot in tracking a moving target.

Both approaches use closed loop controllers without global states (represented by autonomous differential equations). The controllers have to take into account the physical constraints of the vehicle, first of all the limited lateral acceleration and the bounded curvature. Both constraints are especially important for the extension of these methods to the underwater scenario.

The sensor readings in the experiments have been additionally (artificially) disturbed in order to prove the robustness of the discussed methods.

2. The kinematic model and physical constraints

The model, describing the motion of the cartesian unicycle vehicle is given by

$$\begin{aligned} \dot{x} &= u\cos\phi \\ \dot{y} &= u\sin\phi \\ \dot{\phi} &= \omega \end{aligned} \tag{1}$$

being u the linear velocity in the direction of ϕ and ω the angular velocity (figure 1).

In this article, the point-to-point navigation task is considered, i.e. the vehicle starts at point (x_S, y_S) with heading ϕ_S and should be driven with appropriate u and ω to the goal. Without loss of generality the goal can be chosen to be $(x_G, y_G, \phi_G) = (0, 0, 0)$.

Furthermore, u and ω should not explicitly depend on the time but only on the state variables thereby leading to autonomous differential equations for the state variables.

Brockett's Theorem [3] shows that the stabilization for the system (1) can not be solved, because the number of dimensions spanned by linearly independent vectors is not equal to the number of controls.

On the other hand, if the state itself is not defined at the equilibrium, Brockett's Theorem does not pre-

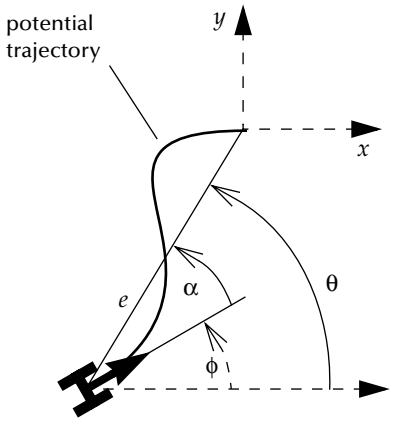

figure 1 : Unicycle kinematic model

vent the stabilization. This can be achieved by a non-linear coordinate transformation.

A suitable choice for this transformation are the following coordinates which were introduced in [1]

$$\begin{aligned} e &= \sqrt{x^2 + y^2} \\ \theta &= \operatorname{atanh}(-y,-x) \\ \alpha &= \theta - \phi \end{aligned} \tag{2}$$

being $\operatorname{atanh}(y,x) \in (-\pi, \pi]$ the four quadrant inverse tangent function describing the angle between a line from (0,0) to (x,y) and the positive x-axis.

With the new coordinates e, α, θ the kinematic model (1) is transformed to (3), on which our further considerations will be based on:

$$\begin{aligned} \dot{e} &= -u\cos\alpha \\ \dot{\theta} &= \frac{u\sin\alpha}{e} \\ \dot{\alpha} &= -\omega + \frac{u\sin\alpha}{e} \end{aligned} \tag{3}$$

Any real vehicle has limitations which depend on the vehicle itself or on its interaction with the environment. The following ones are considered here:

a. bounded linear velocity $u \le u_{max}$

b. bounded angular velocity $\omega \le \omega_{max}$

Normally, the low level motor controllers prevent any dangerous settings of the controls which would break the gears of the vehicle. A more serious problem is the use of control setting ranges which can not be physically realized in the vehicle and would result in an invalid experimental setup.

c. bounded lateral acceleration $a = u \cdot \omega \le a_{max}$

Path tracking experiments depend on the precision of the odometry. If in a curve the lateral acceleration of the vehicle is too strong, the wheels loose close contact to the ground and the odometry data will no longer be meaningful.

d. bounded curvature $c = \frac{\omega}{u} \le c_{max}$

Additionally to the above stated restrictions which apply to every vehicle, a large class of vehicles can not turn on the spot, i.e. the curvature is bounded.

e. only forward moving vehicles $u \ge 0$

Moving is assumed to be possible in one direction only in order to avoid additional bifurcations.

3. Linear velocity Lyapunov approach (LV)

In [1]and [5] it was shown that with the assumption

$$u = \gamma e \qquad \gamma > 0 \tag{4}$$

for the linear velocity and

$$\begin{aligned} V &= \frac{1}{2}(\alpha^2 + h\theta^2) \qquad h > 0 \\ \dot{V} &= -\gamma\beta\alpha^2 \qquad \beta > 0 \end{aligned} \tag{5}$$

for the Lyapunov function and its derivative a non-linear, time-invariant, globally and asymptotically converging control law for ω of the form

$$\begin{aligned} \omega &= \gamma\left(\sin\alpha + \frac{h\theta\sin\alpha}{\alpha} + \beta\alpha\right) \\ & 1 < h \;;\; 2 < \beta < 1 + h \end{aligned} \tag{6}$$

can be found.

Assumption (4) can not be realized on a vehicle because one would get too big velocities or one would have to set γ to a very small value resulting in a very slow motion. Therefore, in experimental setups u will be bounded to u_{max}. It can be shown that even under this condition, the convergence of the system can be preserved.

For practical use the approach has two drawbacks:

- The resulting path scales proportionally in both directions making a very wide side space necessary. (For instance, with a distance of 10 m and the vehicle pointing away from the goal, more than 6 m space to the side are necessary.)
- In order to keep the lateral acceleration in curves bounded to the maximum acceleration, the velocity has to be set to a much smaller value then the vehicle would allow on less curved path segments. The overall speed of this approach is therefore very low.

For this reasons, improvements to the Lyapunov approach and an alternative approach using superimposed dynamics have been looked for.

4. Bounded velocity Lyapunov approach (BV)

While (4) introduced the velocity to depend linearly on the distance, the following assumption for the velocity

$$u = u_{max}\tanh(\kappa e) \tag{7}$$

establishes the existence of an upper bound for the velocity in the Lyapunov approach. Here, κ is a measure for the deceleration of the vehicle when it approaches the goal.

With the same Lyapunov function (5) the angular velocity becomes

$$\omega = u_{max}\left(\frac{\tanh(\kappa e)\sin\alpha}{e} + \frac{h\theta\tanh(\kappa e)\sin\alpha}{\alpha e} + \beta\alpha\right) \tag{8}$$

The convergence to the goal is defined by the behaviour of the solutions for $(e, \theta, \alpha) \rightarrow (0, 0, 0)$. The approximation of the state equations (3) with u and ω from (7) and (8) provide the linearized state equations

$$\dot{e} = -u_{max}\kappa e \tag{9}$$

and

$$\begin{pmatrix}\dot{\alpha}\\ \dot{\theta}\end{pmatrix} = \begin{bmatrix}-\beta u_{max} & -h\kappa u_{max}\\ \kappa u_{max} & 0\end{bmatrix}\begin{pmatrix}\alpha\\ \theta\end{pmatrix} \tag{10}$$

The eigenvalues of the matrix in (10) are

$$\lambda_{1,2} = \frac{u_{max}}{2}(-\beta \pm \sqrt{\beta^2 - 4h\kappa^2}) \tag{11}$$

In order to reach the target on a straight line no oscillations are allowed (i.e. $\beta^2 - 4h\kappa^2 > 0$). Also, the angles (θ, α) must approach zero faster then e. Both is given if the dominant eigenvalue of (11) is strictly larger than the factor governing the decrease of e in (9).

$$u_{max}\kappa < \frac{u_{max}}{2}(\beta - \sqrt{\beta^2 - 4h\kappa^2}) \tag{12}$$

Therefore the conditions for the asymptotic convergence of the bounded velocity approach are

$$1 < h\ ;\ 2\sqrt{h}\kappa < \beta < (1+h)\kappa \tag{13}$$

In order to keep the lateral acceleration bounded to a_{max}, both u and ω are multiplied by a reduction factor $r = \sqrt{a_{max}/u\cdot\omega}$ if $u\cdot\omega > a_{max}$. The curvature and thereby the resulting path is left unchanged.

For large distances, the angular velocity ω in (8) is dominated by the factor $u_{max}\beta\alpha$. In the case of large α, which means the vehicle is pointing away from the goal, ω can not be bounded to an arbitrarily small ω_{max} with a given u_{max} because β has a lower bound given by (13). This contradicting constraints reflect the fact, that one global Lyapunov function and chosen Lyapunov derivative govern very different dynamic situations like turning to the goal, moving toward the goal and converging into the goal.

In order to keep ω bounded, and to preserve the curvature, proportional reduction of both u and ω as in the adjustment of the lateral acceleration is used.

The following parameters have been used in all experiments with the BV approach:

$$\begin{aligned}
&u_{max} = 1.6\ [m/s] && \text{maximal } u\\
&a_{max} = 0.4\ [m/s^2] && \text{max lateral acceleration}\\
&\omega_{max} = 80\ [°/s] && \text{maximal } \omega\\
&h = 2.0\\
&\kappa = 1.0\\
&\beta = 2.9
\end{aligned} \tag{14}$$

Further work should include the bounds on the lateral acceleration and the curvature directly into the Lyapunov approach. One possibility is to introduce an explicit dependency of the velocity u from ω in (7) because it is obvious that the linear velocity of the vehicle should be at its maximum when the vehicle is moving on a straight line, while it should be reduced for curves in order to keep the lateral acceleration bounded.

5. Superimposed Dynamics (SD)

The following approach could be sketched as a superposition of dynamics, where the following aspects are considered and can be formulated individually (e, α, ϕ as introduced above) in the first place:

- *Approaching the goal directly*:
  Far from the goal, only the difference in the heading towards the goal α is considered to control the vehicle with:

$$\omega = \omega_{max}\tanh\left(\frac{c_w\alpha}{\omega_{max}}\right) \tag{15}$$

$$u = u_{max}(u_{min} + (1-u_{min})_{max}\{0, \cos\alpha\}^{c_l}) \tag{16}$$

- *Approaching the goal with specific orientation:*
  Closer to the goal, the trajectory needs to consider the difference to the requested final orientation ϕ as well as the distance to the goal e with:

$$\delta_{close} = c_m\frac{\pi}{2}\tanh\left(\frac{\alpha+\phi}{1-c_m}\right) \tag{17}$$

approximating the direction to a point on the negative x-axis in distance $c_m e$ from the goal, which would be precisely for $|\alpha| < \pi/2$:

$$\operatorname{atan}\left(\frac{c_m\sin\alpha}{1-c_m\cos\alpha}\right) \tag{18}$$

The derived control equations are:

$$\omega = \omega_{max}\tanh\left(\frac{c_\omega(\delta_{close}+\alpha)}{\omega_{max}}\right) \quad (19)$$

$$u = u_{max}\tanh(ec_b) \quad (20)$$

- *At the goal:*
  When so close to the goal that the uncertainties in the positioning are of the same dimension than the actual remaining distance, the direction to the goal is no longer influencing the dynamics. This is especially important, if large changes in α (which are unavoidably increasing as the goal gets closer) should not lead to arbitrary large changes and thus instabilities in ω. Thus the control laws at the goal consider ϕ and e only:

$$\omega = \omega_{max}\tanh\left(\frac{-c_\omega\phi}{\omega_{max}}\right) \quad (21)$$

$$u = u_{max}\tanh(ec_b) \quad (22)$$

  Note that these final approach strategy is *not* reaching the goal exactly, but offers a stable way to get close to the goal only.

By superimposing these aspects of the control task, a closed representation can be formulated, where the robustness of the simple individual parts are preserved. One related method, superimposing dynamics separated in activation and target dynamics can be found in [6]. Another superpositioning method based on connectionist techniques is introduced in [4].

First the currently required deviation δ from the direct heading to the goal is expressed with:

$$\delta = c_m\frac{\pi}{4}\tanh\left(\frac{\alpha+\phi}{1-c_m}\right)\cdot(1-\tanh(c_s(e-c_d))) \quad (23)$$

where c_m gives the strength which attracts the vehicle to a straight line into the goal (i.e. the smoothness or precision of the trajectory can be controlled here), c_d sets the distance at which the intended goal orientation is started to be considered, and c_s gives the speed of the transition from 'straight towards the goal' to the 'final approach' behaviour.

Second the linear velocity reduction and the transition to the relaxed 'being there' dynamic of the control can be formulated as:

$$u_{fo} = 1-(\alpha_d(1-\tanh(ec_b))) \quad (24)$$

$$a_{fo} = 1-(\alpha_d(1-(\tanh(ec_a))^6)) \quad (25)$$

where

$$\alpha_d = {}_{max}\{0, \cos((2\alpha/3)^4)\} \quad (26)$$

Finally the closed control laws for ω and u can be defined as:

$$\omega = \omega_{max}\tanh\left(\frac{\omega_{amp}\delta_o}{\omega_{max}}\right) \quad (27)$$

$$u = u_{max}u_{fo}\tanh\left(\frac{a_l}{|\omega|u_{max}}\right) \quad (28)$$

where

$$\delta_o = a_{fo}(\delta+\alpha+\phi)-\phi \quad (29)$$

The parameter a_l determines the tolerated lateral acceleration. Equation (24) and (25) reflect the fact that deceleration and relaxation is only reasonable, when the goal is in front of the vehicle, where c_a and c_b control the angular relaxation and the linear deceleration respectively. The parameter ω_{amp}, u_{max} and ω_{max} are the overall velocity amplifications and limits.

This approach has no singularities (beside the obvious bifurcation, when the goal is exactly behind the vehicle) and can be adjusted according to the physical constraints of the setup directly. The vehicle will be lead only close to the goal considering the uncertainties of the available position information. Therefore instabilities due to overestimations of the position reliability or precision are avoided. Parameters chosen for the physical experiment are:

$u_{max} = 1.6$	$[m/s]$	maximal u
$\omega_{max} = 60$	$[°/s]$	maximal ω
$\omega_{amp} = 3$	$[1/s]$	amplification in ω
$c_a = 10$	$[1/m]$	angular relaxation
$c_b = 1$	$[1/m]$	deceleration
$c_m = 0.6$	$[0, 1]$	smoothness of final turn
$c_d = 2$	$[m]$	starting final approach
$c_s = 0.5$	$[1/m]$	smoothness of bending away
$a_l = 0.4$	$[m/s^2]$	max lateral acceleration

6. Experimental setup

The physical system employed for all experiments offers the following sensor systems and actuators:

- *3-axis gyroscope*: stability: $\approx 1°/s$; sampling frequency: $176Hz$.
- *3 linear accelerometers*: resolution: $5mG$; sampling frequency: $176Hz$.
- *2 encoders*: resolution: $\approx$ 86000 ticks per wheel revolution; sampling frequency: $58Hz$
- 4 wheel drive with *differential steering*, a maximal linear speed of $\approx 1.6m/s$ and a maximal angular speed of $\approx 150°/s$; control frequency: $193Hz$.

Gyroscopes, accelerometers and encoders are combined to stabilize for glitches in the encoders (wheel slip) and drifts in the gyroscopes. Since the robustness of the approaches against uncertainties is to be proven the resulting position measurement is deteriorated by adding $\pm 10mm/sample$ uniform noise on the linear forward movement and $\pm 3°/sample$ uni-

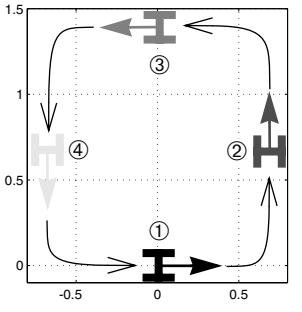

Figure 2a: Forward chained goals

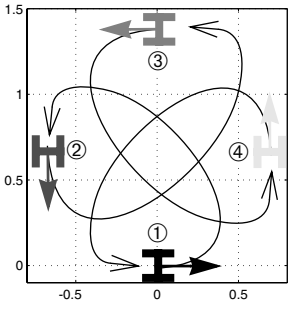

Figure 2b: Backward chained goals

form noise on the orientation information, as measurement by the encoders.

The setup of the experiments has been guided by the long term research goal of using the closed loop controllers in autonomous systems. In such systems discontinuities can be expected due to localization glitches or inconsistencies during local spatio-temporal model updates. The tracking mechanism should react as smooth as possible to this discontinuous changes in the goals of the overall system.

The only assumption in the approaches described above is, that a certain corridor from the start to the goal and a turning space around the goal is not occupied by obstacles. Experiments which are easily reproducible and comparable to other systems and methods can be realized by a cyclic change of goals where the timing of these goal changes has a great impact on the dynamic properties of the robot.

One single goal is defined by the position in space and the orientation of the robot when driving into this position. For each experiment an ordered set of four goals is defined which are approached in a cyclic manner.

The relative change of position and orientation between all adjacent goals are chosen the same in order to avoid limit circles in the dynamic behaviour which are artificially introduced by periodically varying goals. The decision when to change to a new goal is triggered either after a fixed time interval or by the distance to the present goal as measured by the inertial system and the dead-reckoning of the robot.

The goals can be chained forward or backward as shown in figure 2a. In the following experiments backward chained goals are analysed only. These experiments disclose a richer dynamics compared to the forward shifted goal. If the system shows stable behaviour for the case of the backward chained goal, it will be also stable for the case of the forward chained goal but not vice verca.

For all following experiments the next goal relative to the current goal as viewed from the center of the robot is defined as in figure 2b.

6-1. SD - Timed moving goal

Considering robustness as the main aspect of this article, the results in this section are interpreted due to predictability under real world influences. Specifically, it is evaluated whether the tracking system behaves similar in similar situations.

Figure 3a shows the simple case in which the goal is switched slowly (every 6 s). Therefore the tracking system follows synchronously. As soon as the switch time is less than a critical limit at which all four goals may not be approached individually any longer, the tracking system turns to several cyclic behaviours. A significant variance in the peak speeds and the actual tracks can be observed in the *x*-*y* tracks (figure 3b-c) or the u , ω plots (figure 4b-c). Nevertheless cyclic attractors are established, demonstrating that small changes in physical situations are not influencing the global tracking behaviour even if the goals may no longer be actually approached. The wide variety of the individual (but similar) tracks due to unpredictable disturbances and the robust overall motion pattern becomes especially obvious in figure 3b.

Reducing the switch time even further, the state of cyclic attractors is left finally, leading to the state of stochastical reorientation towards quickly changing goals (figure 3d, figure 4d). The covered space as well as the occurring speeds and acceleration are nevertheless strictly bounded, ensuring that even in this case the tracking system keeps well behaved.

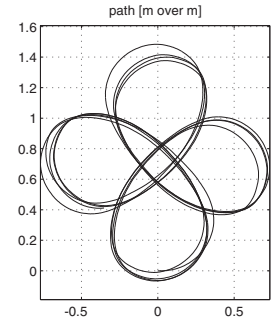

Figure 3a: Switch time 6 s

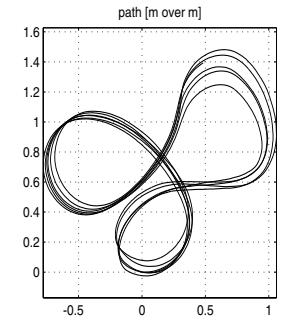

Figure 3b: Switch time 5 s

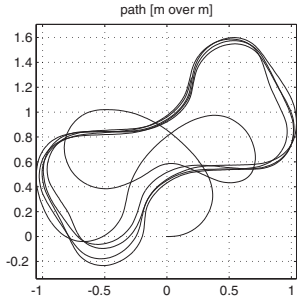

Figure 3c: Switch time 4 s

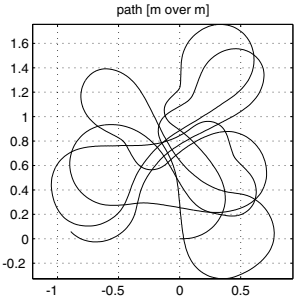

Figure 3d: Switch time 3 s

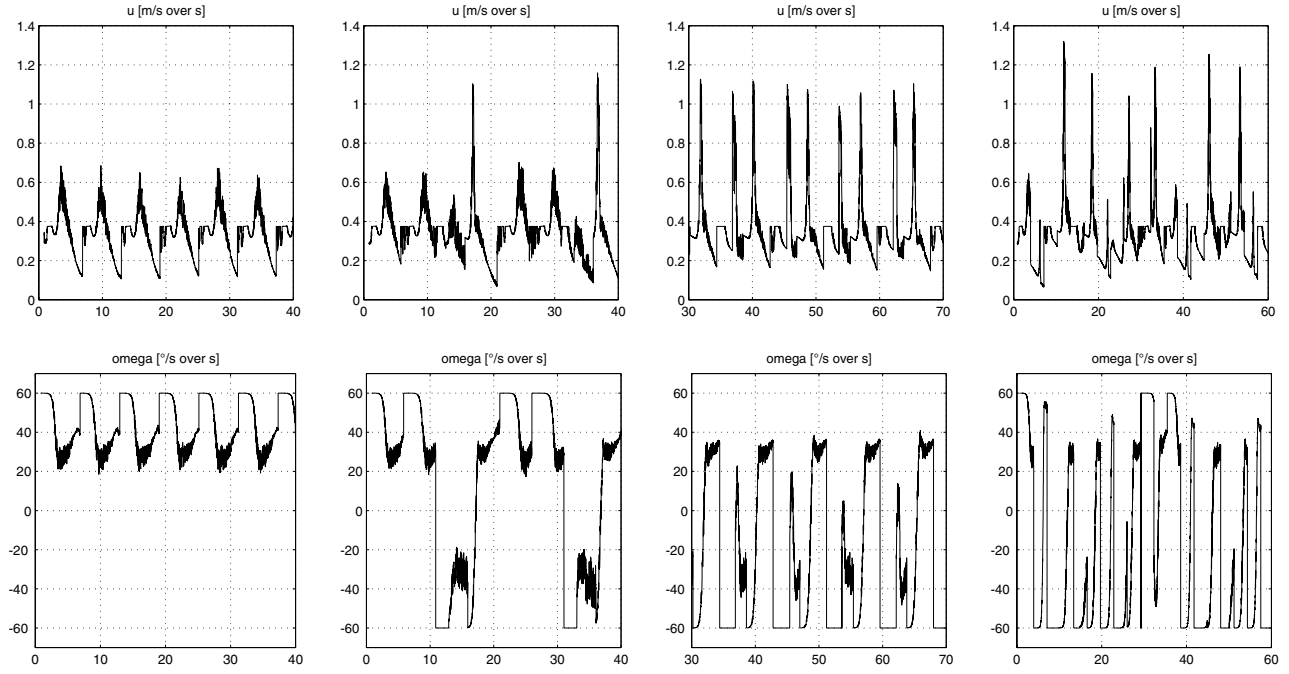

Figure 4a: Switch time 6 s

Figure 4b: Switch time 5 s

Figure 4c: Switch time 4 s

Figure 4d: Switch time 3 s

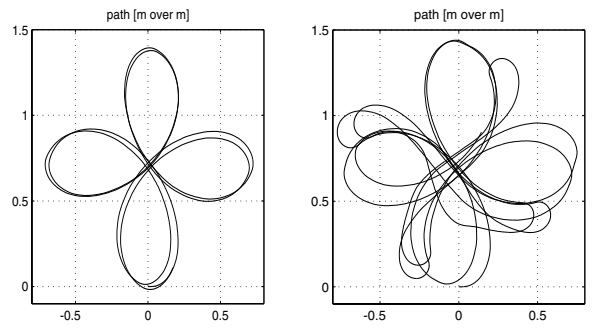

Figure 5a: Switch time 5 s

Figure 5b: Switch time 4 s

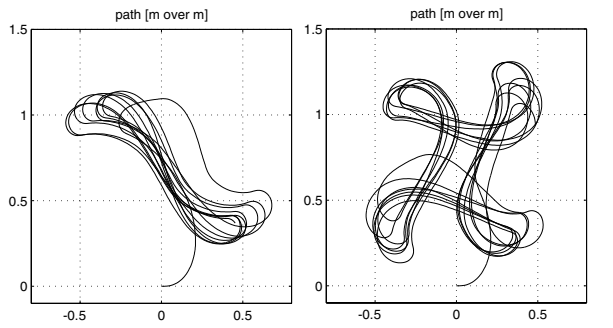

Figure 5c: Switch time 3 s

Figure 5d: Switch time 2 s

6-2. BV - Timed moving goal

The BV method manages a faster turn to the goal compared to the SD approach which results in a larger curvature around the goal points as shown in figure 5a.

With a smaller switch time (figure 5b) two different phases emerge depending on the current attitude of the robot. In case the robot is already close to the goal when the next goal is presented, the phase is the same as in figure 5a. But if the robot is not yet close enough to the current goal the new presented goal is approached with a turn to the right. This takes a certain time and before the robot can really move close to that goal the next goal is presented which the robot is now able to closely approach in time. Which of the two phases are realized depends on the exact conditions where the bifurcation appears and is stochastical in nature.

With yet smaller switch time only the second of the just described phases can be observed (figure 5c). Further reduction of the switch time leads yet to another phase (figure 5d).

Very similar to the results from the SD method, in all cases explored the covered space as well as the velocities and accelerations are strictly bounded and the tracking system is well behaved.

In highly dynamic situations, the BV method constraints (u_{max} , ω_{max} , a_{max}) result in regulating mostly the velocity u and keeping ω at its maximum as shown in figure 6a-b. The SD methods employs both u and ω (see figure 4a-d).

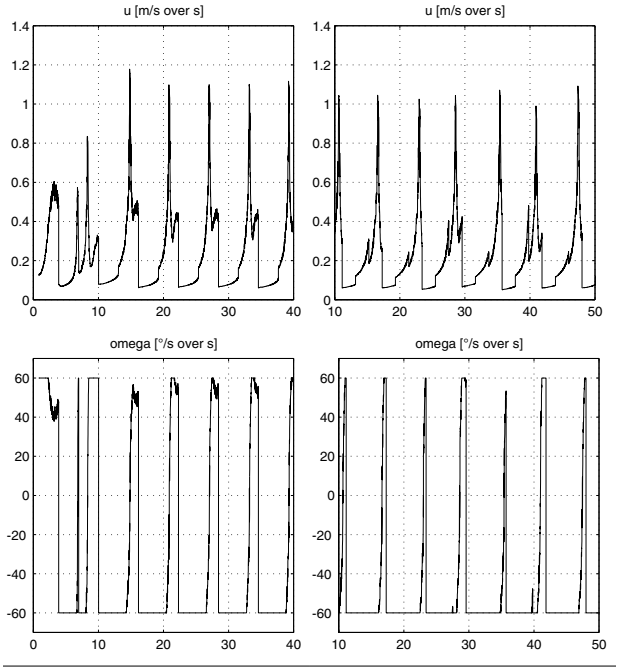

Figure 6a: Switch time 3 s *Figure 6b:* Switch time 2 s

6-3. Effect of noise

All experiments presented up to here are subject to strong disturbances partly from physics, partly from added noise on several channels. In this section the effect of the additional noise is discussed briefly. Enlarging the middle section of the stable tracking in figure 3a, it can be seen in figure 7a that there is a noticeable variance in the actual tracks, but each individual track is smooth and (as discussed before) the overall behaviour is still identical. By removing the artificial noise and performing the experiments due to physical constraints only, figure 7b demonstrate that the variance in the tracks is reduced and the tracks themselves are even smoother. Nevertheless, an effect on the overall behaviour (bifurcations or differences amplified over time) could never be observed.

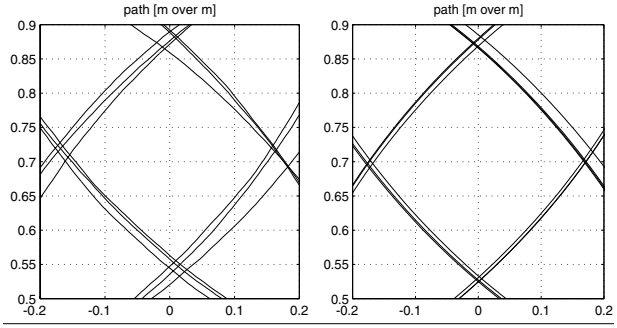

Figure 7a: With artificial noise *Figure 7b:* Without artificial noise

7. Conclusion

The dynamic behaviour and the robustness of two closed loop control methods for track control under real world constraints have been tested. Both methods are stable in a broad range of dynamic situations. The computational complexity of the methods is O(1) which makes them very suitable for fast closed loop control.

The resulting paths and dynamics are very different for both methods, when pushing the test constraints to the limit, while keeping a well-behaved, robust behaviour. By which means these differences have an impact on the overall navigation abilities of autonomous robots, is part of the investigation towards better general navigation evaluation criteria.

References

[1] M. Aicardi, G. Casalino, A.Bicchi, and A. Balestrino
Closed Loop Steering of Unicycle-like Vehicles via Lyapunov Techniques
IEEE Robotics and Automation Magazine, March 1995, pp. 27-35

[2] A. Astolfi
Discontinuous control of nonholonomic systems
Systems & Control letters, vol. 27, pp. 37-45, 1996

[3] R.W. Brockett, R.S. Millmann, and H.J. Sussmann, eds.
Differential Geometric Control Theory
ch. Asymptotic Stability and Feedback Stabilization, by Brockett, R.W., pp. 181-191. Birkhauser, Boston, USA, 1983

[4] Rodney A. Brooks, Paul A. Viola
Network Based Autonomous Robot Motor Control: from Hormones to Learning
Advanced Neural Computers / R. Eckmiller (Editor), Elsevier Science, Publishers B.V. (North-Holland), 1990

[5] G. Indiveri
Kinematic Time-invariant Control of a 2D Nonholonomic Vehicle
38th Conference on Decision and Control, CDC'99, Phoenix, USA, December 1999.

[6] H. Jaeger
The Dual Dynamics Design Scheme for Behaviour-based Robots: a Tutorial
GMD Technical report #966, St. Augustin, Germany 1996 (23 pp.)

[7] M. Krstić , I. Kanellakopoulos, P. Kokotović
Nonlinear and Adaptive Control Design
John Wiley & Sons, Inc., New York 1995.

[8] J.-P. Laumond (ed.)
Robot Motion Planning and Control
Lecture Notes in Control and information Sciences 229, Springer, 1998.